Longitudinal Coupling Impedance of a Cavity*

I. Gjaja and R. L. Gluckstern
Department of Physics, University of Maryland, College Park, MD 20740

Abstract

We conduct a numerical and analytical study of the longitudinal coupling impedance of a cavity coupled to a beam pipe. The aim of the study is to understand the structure of oscillations of the impedance at high frequency.

INTRODUCTION

There exists an integral equation whose solution describes the behavior of the longitudinal coupling impedance for an azimuthally symmetric obstacle in a circular beam pipe [1]. This equation was the starting point for an analysis that led to an explicit expression for the average behavior of the impedance of a cavity at high frequency [1].

In this paper we describe a numerical solution of the integral equation for the pillbox cavity. The results are compared and found to be in agreement with earlier computations of the impedance that are based on different equations [2,3]. We also confirm the above–mentioned explicit expression for the impedance. Finally, we derive an approximate analytical expression that attempts to account for rapid oscillations at high frequency. While the frequency of oscillations is predicted correctly by our model, the amplitude of oscillations does not agree with numerical results.

NUMERICAL RESULTS

The starting point is the equation [1]

$$\int_0^g dz'\, G(z')[K_p(z'-z)+K_c(z',z)] = -\frac{2i\pi}{a} \qquad (1)$$

for the unknown function $G(z)$, which is related to the impedance $Z(k)$ by

$$\frac{Z(k)}{Z_0} = \frac{1}{2\pi ka}\int_0^g dz\, G(z). \qquad (2)$$

(We use e^{-ikct} for the time dependence, in contrast to e^{jkct} used in ref. 1.) Here $K_p(z'-z)$ is the pipe kernel,

$$K_p(z'-z) = \frac{-2i\pi}{ka^2}e^{ik(z'-z)}\sum_{s=1}^{\infty}\frac{e^{ik\sqrt{1-j_s^2/(k^2a^2)}|z'-z|}}{\sqrt{1-j_s^2/(k^2a^2)}}, \qquad (3)$$

where j_s are the zeroes of $J_0(x)$, and $K_c(z',z)$ is the cavity kernel, which in the case of the pillbox cavity can be written in the form

$$K_c(z',z) = \frac{4\pi}{kag}e^{ik(z'-z)}\sum_{n=0}^{\infty}\frac{\cos(\frac{n\pi z}{g})\cos(\frac{n\pi z'}{g})}{(1+\delta_{n0})\sqrt{1-(\frac{n\pi}{kg})^2}}\times \frac{P_1(ka\sqrt{1-(\frac{n\pi}{kg})^2})}{P_0(ka\sqrt{1-(\frac{n\pi}{kg})^2})}. \qquad (4)$$

(Compared to equation (3.12) of ref. 1. we have performed the summation over m.) The symbols $P_1(kay)$ and $P_0(kay)$ stand for

$$P_1(kay) = Y_1(kay)J_0(kby) - J_1(kay)Y_0(kby) \qquad (5)$$

and

$$P_0(kay) = Y_0(kay)J_0(kby) - J_0(kay)Y_0(kby). \qquad (6)$$

In the expressions (1-6) a denotes the radius of the beam pipe, b the radius of the cavity, g the longitudinal extent of the cavity, and Z_0 the impedance of free space, $Z_0 = 120\pi\Omega$.

In order to solve equation (1) numerically, we Fourier transform it on the interval $[0,g]$, thus replacing the continuous indices z and z' by a pair of discrete indices p and q. The transformed equation reads

$$\sum_{p=-\infty}^{\infty}\tilde{G}_p\tilde{K}_{pq} = -\frac{2\pi i}{a}\delta_{q0}, \qquad (7)$$

where the tilde denotes the Fourier transform. In particular, $\tilde{K}_{pq}$ is the sum of Fourier transforms of the cavity and pipe kernels. (The expression is cumbersome and we do not display it here.) The impedance is now given simply by

$$\frac{Z(k)}{Z_0} = -\frac{i}{ka^2}\tilde{K}^{-1}_{00}. \qquad (8)$$

Thus all we need to do numerically is to construct the matrix $\tilde{K}_{pq}$ and then to invert it. In order to ascertain that the result is stable, we vary the size of the matrix $\tilde{K}_{pq}$, as well as the upper limits on the sums in equations (3) and (4). (The upper limits on the sums are chosen such

*Work supported by the U. S. Department of Energy.

0-7803-1203-1/93$03.00 © 1993 IEEE

that for a given size of the matrix $\tilde{K}_{pq}$ all singularities in the sums are included. Except for Figures 1 and 2, where it is smaller, the matrix $\tilde{K}_{pq}$ ranges in size from 81×81 to 121×121.)

Figures 1 and 2 show the real and the negative of the imaginary part of the impedance as functions of ka for $g/a = 0.05$ and $b/a = 1.1$. These are the same values of parameters as used in Figure 6 of reference 2. The results displayed here are in agreement with those of reference 2.

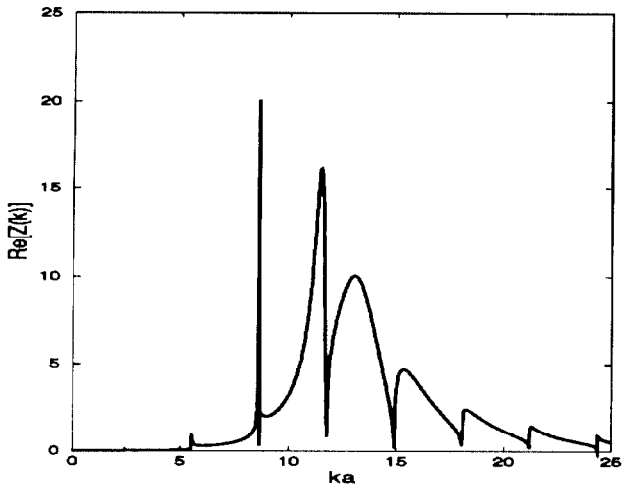

Figure 1: $\mathrm{Re}[Z(k)]$ vs. ka for $b/a = 1.1$ and $g/a = 0.05$.

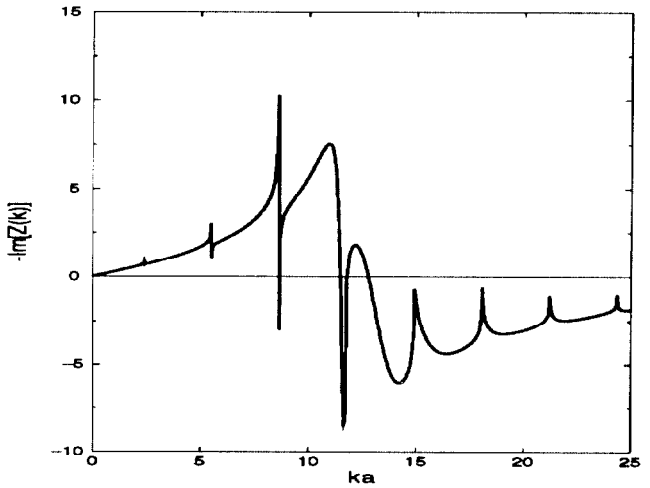

Figure 2: $-\mathrm{Im}[Z(k)]$ vs. ka. Same parameters as Fig. 1.

Our primary interest in this paper is to examine the behavior of $Z(k)$ at high frequency, that is for $ka \gg 1$ and $kg \gg 1$. In this regime, we have compared our results to those obtained in reference 3 and found the two computations to be in agreement.

Figure 3 shows a typical run for $b/a = 1.15$ and $g/a = 0.75$. Superposed on the numerical result is the analytical expression for the average behavior of impedance at high

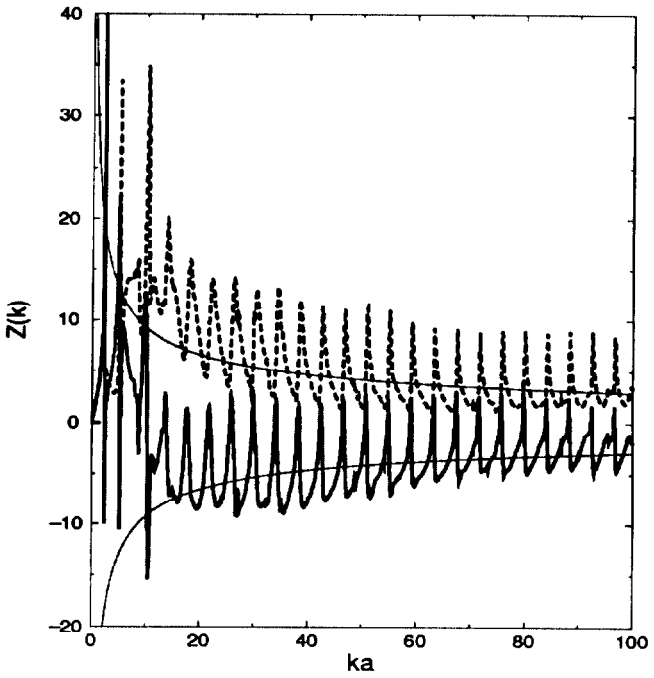

Figure 3: The real part (dashed line) and the negative of the imaginary part (solid line) of $Z(k)$ vs. ka. The thin solid line is the graph of expression (9).

frequency [1]

$$\frac{Z(k)}{Z_0} = \frac{(1+i)}{2\pi a}\sqrt{\frac{g}{\pi k}}. \tag{9}$$

We see that this expression is in satisfactory agreement with the numerical result. Nevertheless, even at large values of ka the behavior of $Z(k)$ is considerably more complicated than $1/\sqrt{k}$. There are large oscillations with an amplitude comparable to the average value of $Z(k)$.

In order to elucidate the structure of the oscillations, we compute the Fourier transform of $\sqrt{k}Z(k)$ for $ka \geq 40$ (using an FFT algorithm). The absolute value of the Fourier transform of Figure 3 multiplied by $\sqrt{k}$ vs. z/a is shown in Figure 4. Apart from the fact that the Fourier transform of $\sqrt{k}Z(k)$ is approximately zero at positive values of z (as it should be by causality), the most striking feature of Figure 4 are the sharp peaks of the graph at the values of $-z$ of $2g, 4g, 6g, \ldots$. Therefore, for large values of ka, $Z(k)$ has oscillations with periods corresponding to $\Delta k = \pi/(ng)$, $n \geq 1$. The amplitude of oscillations decreases with frequency.

Motivated by equation (9) and Figure 4, we can surmise that $\sqrt{k}Z(k)$ is of the form

$$\sqrt{k}Z(k) = \sum_{n=0}^{\infty} \alpha_n e^{-2ink g}, \tag{10}$$

where the α_n's are independent of k. The integral under each of the peaks in Figure 4 then gives the value of $|\alpha_n|$. In Figure 5 we plot the integrals under the peaks vs. n for

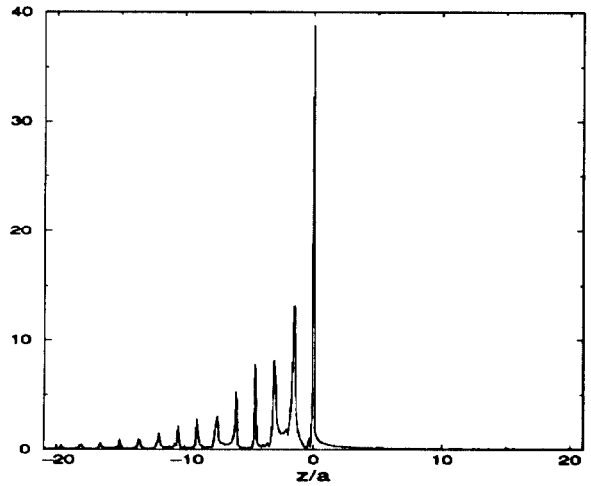

Figure 4: The absolute value of the Fourier transform of $k^{1/2}Z(k)$ vs. z/a; $b/a = 1.15$ and $g/a = 0.75$.

three different values of b. For comparison, we also plot the number $60\sqrt{2g/(\pi a^2)}$, which is the value of $|\alpha_0|$ obtained from equation (9).

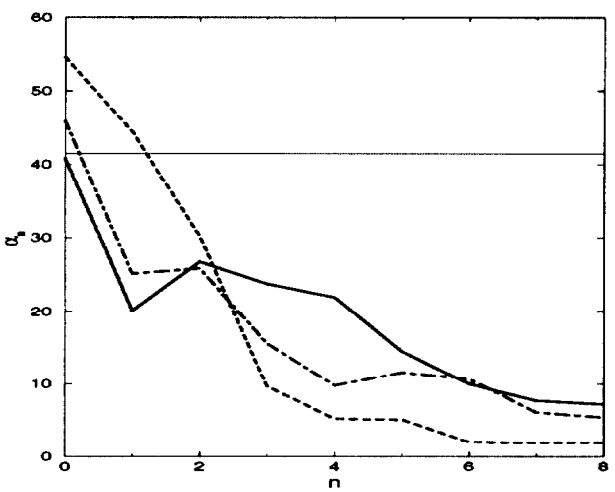

Figure 5: α_n vs. n for b/a =1.1 (dashed line), 1.2 (dash-dot), and 1.5 (solid line). Also shown is the value of α_0 obtained from equation (9) (thin solid line).

From Figure 5 we see that α_n's in general depend on b/a. (With increasing b/a α_0 approaches the solid line, but the Fourier spectrum analogous to the one in Figure 4 becomes increasingly complicated for nonzero negative values of z. We have observed this trend for values of b/a up to 5.) We are currently conducting additional studies to explore the dependence of α_n's on b/a and g/a.

ANALYTICAL RESULTS

We begin the track towards an analytical expression for $Z(k)$ by manipulating the pipe and cavity kernels. Under the assumption that $ka/\pi \gg 1$, K_p can be written in the form

$$K_p(z'-z) \simeq -\frac{i\pi}{a}e^{ik(z'-z)}H_0^{(1)}(k|z'-z|), \qquad (11)$$

where $H_0^{(1)}(x)$ is the Hankel function of the first kind. For $K_c(z',z)$ on the other hand, we use the large-argument asymptotic expansions for P_1 and P_0, and invoke the assumption that $k(b-a)/\pi \gg 1$ to get

$$K_c(z',z) \simeq -\tfrac{i\pi}{a}e^{ik(z'-z)} \times$$
$$\Big[H_0^{(1)}(k|z'-z|) + H_0^{(1)}(k(z+z')) +$$
$$\textstyle\sum_{l=1}^{\infty}[H_0^{(1)}(k(2lg+z-z')) + H_0^{(1)}(k(2lg-z+z')) +$$
$$H_0^{(1)}(k(2lg+z+z')) + H_0^{(1)}(k(2lg-z-z'))]\Big]. \qquad (12)$$

It is worthwhile to note that the dependence of K_c on b has disappeared at this stage and so our final expression for $Z(k)$ will be also independent of b. Next, we use the expressions above for K_p and K_c in equation (1), replace the Hankel functions by their large-argument asymptotic expansions, take $G(z')$ of the form

$$G(z') = \frac{A}{\sqrt{z'}} + \frac{B}{\sqrt{g-z'}}e^{-2ikz'}, \qquad (13)$$

neglect integrals involving fast-oscillating terms, and replace z and z' by $g/2$ in denominators where they occur summed with $2lg$ ($l \geq 1$), to get

$$\frac{Z(k)}{Z_0} = \frac{1}{2a}\sqrt{\frac{g}{\pi k}}(1+i)\Big[\frac{\pi+\lambda(kg)}{\pi^2+(2\pi-1)\lambda(kg)}\Big]. \qquad (14)$$

Here

$$\lambda(kg) = \sum_{l=1}^{\infty}\frac{e^{i2klg}}{\sqrt{2l}}. \qquad (15)$$

The average over oscillations in equation (14) reproduces the result in equation (9). The oscillations in k, on the other hand, occur with period $\Delta k = \pi/(ng)$, $n \geq 1$, which is in agreement with numerical computations. The limitations of equation (14) are that it is independent of b, which, as we have seen, does not agree with numerical results, and that the amplitudes of oscillation, α_n, are much smaller than the ones observed in simulations for $1.05 \leq b/a \leq 5$. We are currently developing an analytical expression for $Z(k)$ that will remove some of the simplifying assumptions built into equation (14).

REFERENCES

1. R. L. Gluckstern, Phys. Rev. D **39**, 2773 (1989).
2. H. Henke, CERN Report LEP-RF/85-41 (1985).
3. R. Li, PhD Thesis, University of Maryland (1990).